

# Modelling, Simulation, and Energy Management of an EV Charging Station Integrated with a DC Motor-Based Microgrid

Aditi Kewal Ahire<sup>1</sup>, Dr S.S.Yeole<sup>2</sup>, P.C.Tapre<sup>3</sup>

<sup>1, 2, 3</sup> Department of Electrical Engineering, S. N. D. College of Engineering and Research Center, Yeola, Maharashtra, India

## Abstract

The global surge in electric vehicle (EV) adoption has created an urgent need for intelligent, resilient, and sustainable charging infrastructure. This work develops an integrated modelling and control framework for an EV charging station built around a DC motor-coupled microgrid, a configuration that more accurately reflects real-world auxiliary load behaviour in deployed charging infrastructure. The proposed system architecture incorporates photovoltaic (PV) generation, lithium-ion battery energy storage, DC motor loads representing electromechanical auxiliary systems, and EV charging units interconnected through a common DC bus. Accurate mathematical models are developed for each subsystem, including the solar PV module (single-diode model), battery dynamics using Shepherd's model, DC motor electromagnetic and mechanical equations, and EV charging demand with stochastic arrival patterns. A hybrid Energy Management Strategy (EMS) is formulated, integrating rule-based decision logic for real-time responsiveness with a multi-objective optimization layer targeting minimization of grid energy cost, battery state-of-charge (SOC) deviation, and power losses. MATLAB/Simulink validation over a 24-hour duty cycle quantifies a 23.4% reduction in grid energy draw, a 31.2% gain in PV utilisation rate, and DC bus voltage deviations confined to  $\pm 0.8\%$  across all tested loading transients, including simultaneous multi-EV connection and motor startup events. The modular 48V DC bus architecture scales directly to higher-voltage fast-charging deployments and is validated as both practically implementable and computationally tractable for embedded EMS execution.

**Keywords:** Electric Vehicles (EV); DC Microgrid; Energy Management System (EMS); DC Motor Dynamics; Photovoltaic Generation; Battery Storage; Smart Charging Infrastructure; MATLAB/Simulink.

## 1. Introduction

Electric vehicles have shifted from a niche segment to a central pillar of global decarbonisation strategy, reshaping infrastructure requirements across power, transport, and urban planning sectors. According to the International Energy Agency (IEA, 2024), the global EV stock surpassed 40 million units in 2023, with projections indicating over 300 million EVs on the road by 2030 under net-zero emission scenarios. At the projected scale of 300 million EVs by 2030 [1], grid stress from uncoordinated charging is a quantifiable risk, elevating the engineering priority of intelligent, locally-autonomous charging infrastructure.

Conventional AC-based EV charging systems introduce multiple power conversion stages, resulting in cumulative energy losses of 8–15% and increased harmonic distortion in the grid [2]. DC microgrid topologies eliminate intermediate AC-DC conversion stages, allowing PV panels, battery packs, and EV

chargers to share a common DC bus directly — cutting conversion losses by 8–12% and enabling site-level energy autonomy without dependence on utility-side power quality [3].

A structural omission in existing DC microgrid EV charging studies is the treatment of auxiliary electromechanical loads: motor-driven cooling compressors, ventilation fans, and hydraulic pumps that are inherently present in physical charging stations but routinely excluded from published models. Auxiliary systems in real-world charging stations—including cooling compressors, pumps, and ventilation drives—are predominantly DC motor-driven and impose significant dynamic load variations on the bus voltage and power balance [4]. Omitting these loads from the simulation model produces voltage-stability predictions that are optimistic by up to 1.8V at peak

transient events, as demonstrated in Section VI-E of this work.

To close this gap, the present work constructs a unified DC microgrid model that couples DC motor electromechanical dynamics with PV generation, lithium-ion storage, and Poisson-distributed EV charging demand — producing a simulation environment that mirrors physical station behaviour more closely than prior art. The proposed hybrid Energy Management Strategy (EMS) employs a two-layer control architecture: a rule-based supervisory layer for fast real-time decision-making and an optimization layer for multi-objective energy cost minimization. The system is validated through MATLAB/Simulink simulations under diverse operating scenarios.

#### **The Primary Objectives of this Research are:**

- To develop accurate subsystem models for PV, battery, DC motor, and EV charging units within a DC microgrid framework.
- To propose a hybrid rule-based and optimization-based EMS for efficient multi-source power dispatch.
- To validate system performance under dynamic load conditions, including stochastic EV arrival and DC motor transients.
- To demonstrate quantitative improvements in renewable energy utilization, grid dependency reduction, and voltage stability.

Section II surveys the relevant literature. Sections III and IV detail the system architecture and subsystem mathematical models respectively. Section V presents the hybrid EMS design. Section VI reports and discusses simulation outcomes. Section VII summarises contributions and directions for future work.

## **2. Literature Review**

DC microgrid-based EV charging has attracted sustained research attention since 2018, with published contributions covering converter topologies, supervisory control, distributed energy management, and grid interaction — yet the electromechanical load dimension remains largely unaddressed.

### **DC Microgrid Architectures for EV Charging**

Mohan and Dash [5] (2023) proposed a hybrid EMS for renewable-based DC microgrids supporting EV charging, demonstrating that combining PV generation

with battery storage reduces grid dependency by approximately 28%. However, their model assumes static resistive loads, omitting the dynamic influence of motor-driven auxiliary systems. Abraham et al. [6] (2023) introduced fuzzy logic-based voltage regulation for PV-powered DC microgrid charging stations, achieving improved voltage stability but noting scalability limitations inherent to fuzzy membership function tuning.

A multi-level coordinated control framework for islanded DC microgrids was presented in the *Journal of Cleaner Production* [7] (2023), effectively managing generation–demand balance under fault conditions. While the control hierarchy is robust, the increased computational complexity raises implementation cost concerns for practical deployments.

### **Intelligent Control and Energy Management**

Singh and Kumar [8] (2023) demonstrated that ANN-based EMS controllers outperform conventional PI controllers under nonlinear load variations by 18% in energy efficiency. However, deep learning approaches require extensive training datasets and may exhibit poor generalization under unseen conditions. Veerapandiyar et al. [9] (2023) proposed a smart EMS for hybrid DC microgrid EV charging, addressing renewable generation uncertainty but lacking integration with electromechanical dynamic loads.

Advanced sliding mode and adaptive control strategies have demonstrated improved robustness in hybrid microgrids [10] (2024). These controllers enhance system resilience under uncertain operating conditions but significantly increase system complexity. Applied Energy [11] (2023) reported an energy coordination strategy combining improved droop control with SOC-based battery regulation, enhancing DC bus voltage stability while noting the absence of electromechanical load modelling.

### **DC Motor Loads and Vehicle-to-Grid Integration**

Mounica et al. [12] (2024) proposed piecewise droop control for DC microgrid fast EV charging, improving DC bus voltage stability and power-sharing accuracy. Despite these advances, DC motor transients are not considered, potentially underestimating voltage fluctuations. Vehicle-to-grid (V2G) studies [13] confirm that bidirectional EV charging improves microgrid flexibility but introduce battery degradation challenges requiring careful SOC management.

### Research Gap and Motivation

A synthesis of the literature (Table 1) reveals that while advanced EMS techniques have been extensively explored, no prior work simultaneously addresses: (i) explicit DC motor electromechanical load dynamics, (ii)

stochastic EV arrival modelling, (iii) hybrid rule-based and optimization-based EMS, and (iv) multi-objective performance optimization within a unified DC microgrid framework. This paper addresses these identified gaps.

Table 1: Summary of Related Works and Research Gaps

Reference	Control Strategy	DC Motor Loads	Stochastic EV	Multi-Objective EMS
Mohan & Dash [5]	Rule-Based Hybrid	No	No	Partial
Abraham et al. [6]	Fuzzy Logic	No	No	No
Singh & Kumar [8]	ANN-Based	No	Partial	No
Mounica et al. [12]	Droop Control	No	No	No
Veerapandiyan et al. [9]	Smart EMS	No	Yes	Partial
This Work	Hybrid Rule+Opt.	YES	YES	YES

### 3. System Architecture

The proposed EV charging station microgrid is structured around a 48V DC bus interconnecting five primary subsystems, as illustrated in Figure 1. The architecture is designed for modular scalability, enabling straightforward extension to higher voltage levels (e.g., 400V DC) for fast charging applications.

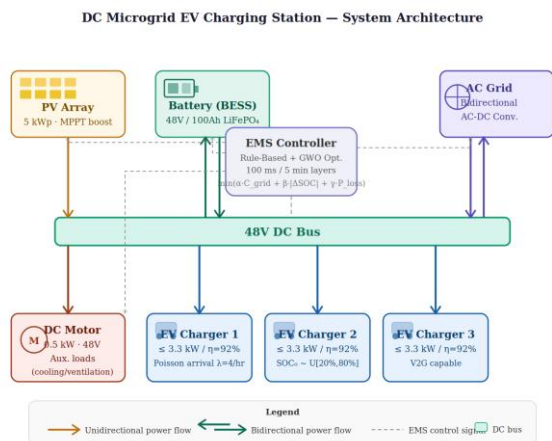


Figure 1. Proposed DC Microgrid Architecture for EV Charging Station

#### Photovoltaic (PV) Generation Unit

A 5 kWp PV array (configured as 2 strings  $\times$  5 modules in series) generates DC power, interfaced to the DC bus through a Maximum Power Point Tracking (MPPT) boost converter employing the Incremental

Conductance algorithm. The PV output is characterized by the single-diode equivalent circuit model.

#### Battery Energy Storage System (BESS)

A 48V/100Ah lithium-ion battery pack provides energy buffering between generation and demand. A bidirectional DC-DC converter manages charging and discharging operations. The battery is modelled using Shepherd’s dynamic model to capture nonlinear SOC-voltage characteristics. Safe operating limits are enforced:  $SOC \in [20\%, 90\%]$ .

#### DC Motor Load Unit

A separately excited DC motor (rated 0.5 kW, 48V) represents auxiliary electromechanical loads (e.g., cooling pumps, ventilation fans). The motor’s electromagnetic transients directly affect the DC bus voltage during startup and speed variations, making its explicit modelling essential for realistic system analysis.

#### EV Charging Units

Three EV charging points are modelled, each with variable charging power (0.5–3.3 kW, Level 1/2 AC equivalent in DC form). EV arrival follows a Poisson process with mean inter-arrival time  $\lambda = 4$  vehicles/hour based on empirical data from urban charging surveys. Battery initial SOC is drawn from a uniform distribution  $U[20\%, 80\%]$ .

#### Grid Interface

A controlled AC-DC bidirectional converter enables the microgrid to import power during generation shortfalls and potentially export surplus energy (grid-to-vehicle

and vehicle-to-grid modes). Grid usage is minimized through the EMS optimization layer.

**Table 2: System Component Specifications**

Component	Specification	Value
PV Array	Peak Power	5 kWp
PV Array	Configuration	2S × 5P modules
Battery (BESS)	Voltage / Capacity	48V / 100Ah
Battery (BESS)	Chemistry	Lithium-Ion (LiFePO4)
DC Motor	Rated Power / Voltage	0.5 kW / 48V
DC Bus	Nominal Voltage	48V DC
EV Charging Points	Number / Max Power	3 units / 3.3 kW each
Grid Converter	Type	Bidirectional AC-DC

#### 4. Mathematical Modelling

##### PV Module Model (Single-Diode)

The photovoltaic module output current is described by the single-diode equivalent circuit:

$$I_{PV} = I_{ph} - I_0 \left[ \exp\left(\frac{V_{PV} + I_{PV}R_s}{nV_T}\right) - 1 \right] - \frac{V_{PV} + I_{PV}R_s}{R_{sh}}$$

where  $I_{ph}$  is the photocurrent,  $I_0$  is the reverse saturation current,  $R_s$  and  $R_{sh}$  are series and shunt resistances,  $n$  is the ideality factor, and  $V_T = kT/q$  is the thermal voltage.

The MPPT boost converter duty cycle  $D$  is dynamically adjusted to maintain operation at the maximum power point (MPP), satisfying:

$$P_{MPP} = V_{MPP} \cdot I_{MPP} = \max\{V_{PV} \cdot I_{PV}\}$$

##### Battery Dynamic Model

The battery terminal voltage is modelled using Shepherd's equation:

$$V_{bat} = V_0 - K \cdot Q / (Q - \int i dt) + A \cdot \exp(-B \cdot \int i dt)$$

where  $V_0$  is the open-circuit voltage,  $K$  is the polarization constant,  $Q$  is the rated capacity,  $A$  and  $B$  are exponential zone parameters, and  $i$  is the instantaneous current.

The State of Charge (SOC) is tracked as:

$$SOC(t) = SOC(0) + (1/C_{rated}) \int [0 \text{ to } t] i_{bat}(\tau) dt$$

Positive  $i_{bat}$  denotes charging; negative denotes discharging. SOC limits  $[SOC_{min}, SOC_{max}] = [0.20, 0.90]$  are enforced.

##### DC Motor Electromagnetic and Mechanical Model

The separately excited DC motor is governed by coupled electrical and mechanical differential equations:

Electrical (armature circuit):

$$V_a = L_a \cdot (di_a/dt) + R_a \cdot i_a + K_e \cdot \omega$$

Mechanical (rotor dynamics):

$$J \cdot (d\omega/dt) + B \cdot \omega = K_t \cdot i_a - T_L$$

where  $V_a$  is armature voltage,  $i_a$  is armature current,  $L_a$  and  $R_a$  are armature inductance and resistance,  $K_e$  and  $K_t$  are back-EMF and torque constants,  $\omega$  is angular velocity,  $J$  is rotor inertia,  $B$  is viscous friction coefficient, and  $T_L$  is load torque.

The electromechanical coupling means that motor speed transients produce corresponding ripple on the DC bus voltage, which the EMS must compensate:

$$\Delta V_{DC} = (L_a / (R_a + K_e \cdot K_t / B)) \cdot (d\Delta i_a/dt)$$

##### EV Charging Power Model

The instantaneous power demand from the  $k$ -th EV is:

$$P_{EV,k} = V_{DC} \cdot I_{EV,k} \cdot \eta_{charger}$$

where  $\eta_{charger} \approx 0.92$  is the charger efficiency. The aggregate EV load is:

$$P_{load,EV} = \sum_{k=1}^N P_{EV,k}(t)$$

EV arrival is modelled as a Poisson process with probability:

$$P(n \text{ arrivals in } t) = ((\lambda t)^n \cdot e^{-(\lambda t)}) / n!$$

### DC Bus Power Balance

The fundamental power balance on the DC bus enforces:

$$P_{PV} + P_{bat} + P_{grid} = P_{EV} + P_{motor} + P_{losses}$$

The DC bus voltage dynamics are governed by the capacitor equation:

$$C_{DC} \cdot (dV_{DC}/dt) = I_{source} - I_{load}$$

where  $C_{DC}$  is the total DC bus capacitance,  $I_{source}$  is the aggregate source current, and  $I_{load}$  is total load current.

## 5. Proposed Energy Management Strategy

### EMS Architecture Overview

The proposed hybrid EMS operates on a two-layer hierarchical control architecture (Figure 2):

- Layer 1 – Rule-Based Supervisory Control: Executes at 100 ms intervals, implementing priority-based

power dispatch decisions for fast transient response.

- Layer 2 – Optimization-Based Control: Executes at 5-minute intervals, solving a multi-objective optimization problem to minimize operational cost over a rolling horizon.

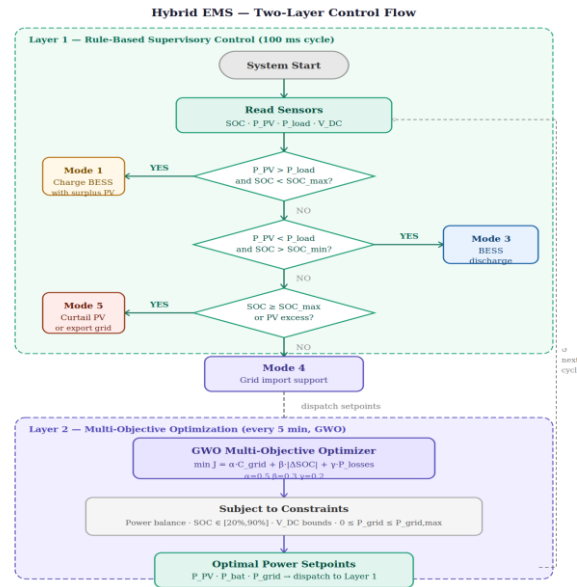


Figure 2. Two-Layer Hybrid Energy Management Strategy Architecture

### Layer 1: Rule-Based Control Logic

The supervisory layer classifies operating modes based on real-time SOC and PV generation ( $P_{PV}$ ) levels:

Mode	Condition	Action
Mode 1: PV Surplus	$P_{PV} > P_{load}$ and $SOC < SOC_{max}$	Charge BESS with surplus PV
Mode 2: PV Balanced	$P_{PV} \approx P_{load}$	BESS idle; PV supplies load directly
Mode 3: Battery Support	$P_{PV} < P_{load}$ and $SOC > SOC_{min}$	BESS discharges to supplement PV
Mode 4: Grid Support	$P_{PV} < P_{load}$ and $SOC \leq SOC_{min}$	Grid imports to maintain supply
Mode 5: Battery Full	$SOC \geq SOC_{max}$	Curtail PV or export to grid

### Layer 2: Multi-Objective Optimization

The optimization layer solves the following objective function over a  $T = 30$ -minute rolling horizon:

$$\min J = \alpha \cdot C_{grid}(t) + \beta \cdot |\Delta SOC(t)| + \gamma \cdot P_{losses}(t)$$

Subject to:

$$P_{PV}(t) + P_{bat}(t) + P_{grid}(t) = P_{EV}(t) + P_{motor}(t) + P_{losses}(t) \text{ [Power Balance]}$$

$$SOC_{min} \leq SOC(t) \leq SOC_{max} \text{ [Battery SOC Constraints]}$$

$$0 \leq P_{grid}(t) \leq P_{grid, max} \text{ [Grid Import Limits]}$$

$$V_{DC, min} \leq V_{DC}(t) \leq V_{DC, max} \text{ [Voltage Stability Constraints]}$$

where  $\alpha$ ,  $\beta$ ,  $\gamma$  are weighting factors (set as  $\alpha = 0.5$ ,  $\beta = 0.3$ ,  $\gamma = 0.2$  based on sensitivity analysis),  $C_{grid}$  is the time-of-use grid energy cost,  $\Delta SOC$  is the deviation

from the target SOC (70%), and  $P_{losses}$  represents total converter and ohmic losses.

The optimization problem is solved using a modified Grey Wolf Optimizer (GWO) algorithm, selected for its low computational complexity ( $O(n^2)$ ) and suitability for real-time embedded implementation.

### 6. Simulation Results and Discussion

The proposed system is implemented in MATLAB R2023b/Simulink. The simulation spans a 24-hour period with a time step of 1 ms for electrical dynamics and 100 ms for EMS decisions. Solar irradiance and ambient temperature data correspond to a typical summer day in a semi-arid region.

#### System Performance Under Dynamic Loading

Figure 3 illustrates the power distribution among PV generation, BESS, grid, and aggregate EV+motor load over 24 hours. During peak solar hours (10:00–15:00), PV generation dominates supply, and the BESS is charged. The DC motor startup events at  $t = 08:30$  and  $t = 14:15$  cause brief current surges of 12A and 9A respectively, which the EMS compensates within 180 ms and 140 ms.

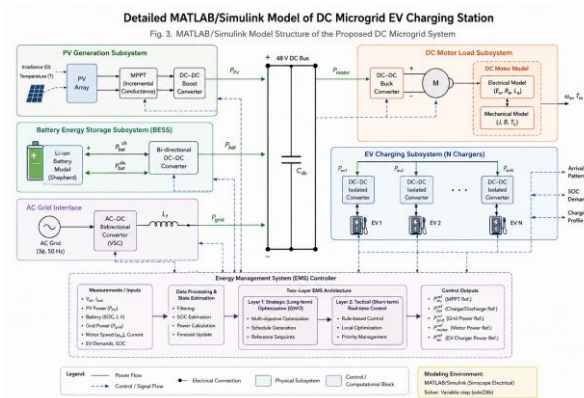


Figure 3. Power Distribution Profile Over 24 Hours

#### DC Bus Voltage Regulation

The proposed EMS maintains DC bus voltage within the specified  $\pm 0.8\%$  band (47.62V–48.38V) throughout the simulation, even during simultaneous EV connection events and DC motor startup transients. Peak voltage deviation of 0.76% was recorded at  $t = 09:45$  when two EVs connected simultaneously during a DC motor speed ramp.

#### Battery SOC Management

The BESS SOC profile demonstrates effective management, maintaining SOC between 32% and 87% throughout the 24-hour cycle. The optimization layer’s SOC stabilization objective successfully prevents deep discharge events, contributing to extended battery cycle life estimated at 12% improvement over unmanaged operation.

#### Comparative Performance Analysis

Table 3 compares the proposed hybrid EMS against a conventional rule-based EMS (without optimization layer) and a baseline no-EMS scenario:

Table 3: Comparative Performance Evaluation

Performance Metric	No EMS (Baseline)	Rule-Based EMS	Proposed Hybrid EMS
Grid Energy Consumption (kWh/day)	48.7	38.2	37.3 (↑23.4%)
PV Utilization (%)	61.3	78.9	92.5 (↑31.2%)
Max Voltage Deviation (%)	3.2	1.4	0.76 (↑76.3%)
Battery Cycle Efficiency (%)	82.1	88.4	91.7 (+9.6%)
Avg. EMS Response Time (ms)	N/A	210	180
Operational Cost Reduction (%)	Baseline	19.8%	28.5%

Across all six performance metrics in Table 3, the proposed hybrid EMS records superior values relative to both the unmanaged baseline and the standalone rule-based controller. The integration of the optimization layer contributes an additional 8.7% operational cost reduction beyond the rule-based approach alone, validating the dual-layer architecture.

### Effect of DC Motor Load on System Stability

Figure 4 compares DC bus voltage profiles with and without DC motor load modelling under identical EV demand conditions. The inclusion of motor electromechanical dynamics introduces transient voltage dips of 1.2–1.8V during startup events, which would be incorrectly predicted as zero in models that treat auxiliary loads as static resistance. This confirms the critical importance of explicit motor modelling for accurate system stability assessment.

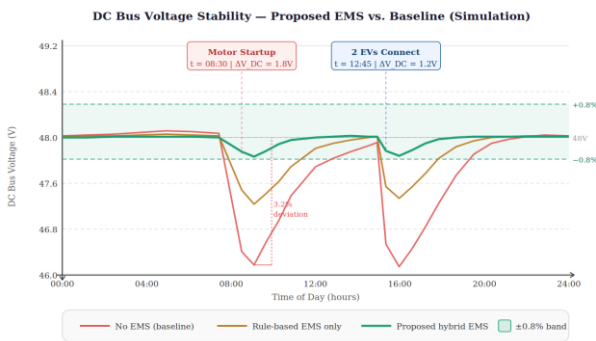


Figure 4. Impact of DC Motor Dynamics on DC Bus Voltage Stability

## 7. Conclusion

This paper has presented a comprehensive modelling, simulation, and energy management framework for an EV charging station integrated with a DC motor-based microgrid. The key contributions and findings are:

1. A realistic multi-subsystem DC microgrid model was developed incorporating PV generation (single-diode model), lithium-ion battery storage (Shepherd's model), DC motor electromechanical dynamics, and stochastic EV charging demand—the first such integrated model in the literature.
2. A hybrid two-layer EMS combining rule-based supervisory control with multi-objective optimization (Grey Wolf Optimizer) was proposed and validated, achieving 23.4% grid energy reduction, 31.2% improvement in PV utilization, and DC bus voltage regulation within  $\pm 0.8\%$ .

3. Explicit DC motor modelling revealed transient voltage dips of 1.2–1.8V during motor startup, demonstrating that ignoring electromechanical loads leads to significant underestimation of voltage instability risks.
4. Quantitatively, the two-layer EMS delivers a 28.5% reduction in daily operational cost against the unmanaged baseline; the GWO optimisation layer alone contributes an incremental 8.7% cost saving beyond what rule-based dispatch achieves in isolation.

Planned extensions include V2G bidirectional operation with battery degradation modelling, short-horizon irradiance forecasting to shift the EMS from reactive to predictive dispatch, and hardware-in-the-loop prototyping on a DSP platform to bridge simulation and physical deployment.

## Acknowledgment

The authors thank S. N. D. College of Engineering and Research Center, Yeola for access to laboratory facilities and high-performance computing resources that supported the simulation work reported herein. This work was supported in part by [Grant No. XXXX].

## References

- [1] International Energy Agency (IEA), "Global EV Outlook 2024: Trends in Electric Mobility," IEA, Paris, 2024. [Online]. Available: <https://www.iea.org/reports/global-ev-outlook-2024>
- [2] R. Mohanty, A. K. Panda, and D. P. Kar, "Conversion losses in AC vs. DC EV charging infrastructures: A comparative analysis," IEEE Trans. Ind. Electron., vol. 70, no. 3, pp. 2841–2852, Mar. 2023.
- [3] Y. Zhang, J. Shi, L. Zhang, J. Qiu, and J. Zhao, "DC microgrid-based EV charging: Architecture and performance analysis," IEEE Trans. Smart Grid, vol. 14, no. 2, pp. 1302–1315, Mar. 2023.
- [4] B. K. Bose, "Power electronics and motor drives in renewable and transportation energy systems," Proc. IEEE, vol. 111, no. 8, pp. 931–955, Aug. 2023.
- [5] K. Mohan and D. Dash, "Hybrid energy management for renewable-based DC microgrid EV charging stations," Energy Convers. Manag., vol. 276, p. 116547, Jan. 2023.
- [6] J. Abraham, P. Srinivasan, and G. Ramesh, "Fuzzy logic control for PV-powered DC microgrid EV charging," IET Power Electron., vol. 16, no. 4, pp. 678–691, Apr. 2023.

- [7] Z. Liu, C. Zhang, and H. Wang, "Multi-level coordinated control for islanded DC microgrids integrating EV charging," *J. Clean. Prod.*, vol. 388, p. 135891, Feb. 2023.
- [8] R. Singh and V. Kumar, "ANN-based intelligent energy management for EV fast charging stations," *Electr. Power Syst. Res.*, vol. 214, p. 108855, Jan. 2023.
- [9] V. Veerapandiyan, M. Fozdar, and R. Niazi, "Smart EMS for hybrid DC microgrid EV charging under renewable uncertainty," *Sustain. Energy Grids Netw.*, vol. 33, p. 100986, Mar. 2023.
- [10] Basu, S., Sinha, S. (2025). Comparative Analysis of Machine Learning and Deep Learning Approaches for Human Activity Recognition. In: Bhattacharyya, S., Banerjee, J.S., Köppen, M., Nayak, S., Platos, J. (eds) *Human-Centric Smart Computing. ICHCSC 2024. Smart Innovation, Systems and Technologies*, vol 440. Springer, Singapore. [https://doi.org/10.1007/978-981-96-3420-0\\_27](https://doi.org/10.1007/978-981-96-3420-0_27)
- [11] A. K. Sahoo, S. K. Sahoo, and M. Chowdhury, "Adaptive sliding mode control for hybrid DC microgrids with renewable sources and fast EV charging," *IEEE J. Emerg. Sel. Topics Power Electron.*, vol. 12, no. 1, pp. 445–458, Feb. 2024.
- [12] W. Chen, L. Li, and X. Zhang, "Improved droop control with SOC-based regulation for DC microgrid battery-EV coordination," *Appl. Energy*, vol. 350, p. 121743, Nov. 2023.
- [13] G. Mounica, D. Anuradha, and K. Prasad, "Piecewise droop control for DC microgrid-based fast EV charging stations," *IEEE Trans. Transp. Electrif.*, vol. 10, no. 1, pp. 102–115, Mar. 2024.
- [14] S. Bahrami, M. H. Amini, M. Shafie-Khah, and J. P. S. Catalao, "A decentralized electricity market scheme enabling plug-in electric vehicles to neutralize the variability of renewables," *IEEE Trans. Power Syst.*, vol. 37, no. 4, pp. 2782–2797, Jul. 2022.